Chapter 5

Characterization of NanoSized Diamond-Like Carbon Emitters Arrays

5.1. Introduction

According to the results of chapter 4, it is believed that diamond materials can be used to improve the performance of field emission. Diamond and diamond-like carbon (DLC) are presently being investigated and applied for use in field emission devices because diamond has negative electron affinity and robust mechanical and chemical properties. The diamond growth process used by researchers to make the devices also varies greatly. Observations of electron emission from chemical vapor deposition (CVD) diamond under relative low electric fields (3-40 v/μm) have been reported [1-3]. Fabrication of diamond field emitter arrays has also been attempted [4] and a diode-structured prototype field emission display based on a diamond-like carbon cathode has been demonstrated [5]. However, it is not entirely clear how the electron emission from these seemingly undoped or p-typed-doped CVD diamonds can occur at such low fields.

Usually, for a semiconductor field emitter, the emitter electrons can originate from either the conduction band, the valence band, and/or surface states. Diamond has a wide band gap with Eg=5.5 eV. In order to induce stable electron field emission from diamond, either the bulk or the surface must first be made conductive. It is believed

that the impurities such as nitrogen, boron or phosphorus can enhance diamond's electron property by offering holes or electrons.

In this chapter, we present a new process to fabricate a new gate structure and smaller gate aperture metal/insulator/semiconductor (MIS) diode, which can shorten the space distance of gate-tip and improve the field emission current density. Phosphorus-doped and boron-doped diamond-like carbon emitters by using trimethylphosphite $P(OCH_3)_3$ and trimethylborate $B(OCH_3)_3$ as doping sources in a microwave plasma chemical vapor deposition system (MWCVD) are synthesized in gated structure. Based on our experimental results from scanning electron microscopy (SEM) and Raman spectra, there is much difference among undoped, phosphorus-doped and boron-doped diamond-like material. In addition, doping both phosphorus and boron can enhance electric properties by reducing the turn-on voltage and can increase the emission current density. The turn-on voltages of undoped, boron-doped and phosphorus-doped emitters in triode-type field emitter arrays are 15V, 8V and 5V, respectively. The emission currents of boron-doped and phosphorus-doped emitters are about twenty and eighty times larger than the undoped.

5.2. Experiment

Figure 5.1 shows the flow chart of experimental procedure. First, we design the MIS diode structure and fabricated the MIS diode by semiconductor process

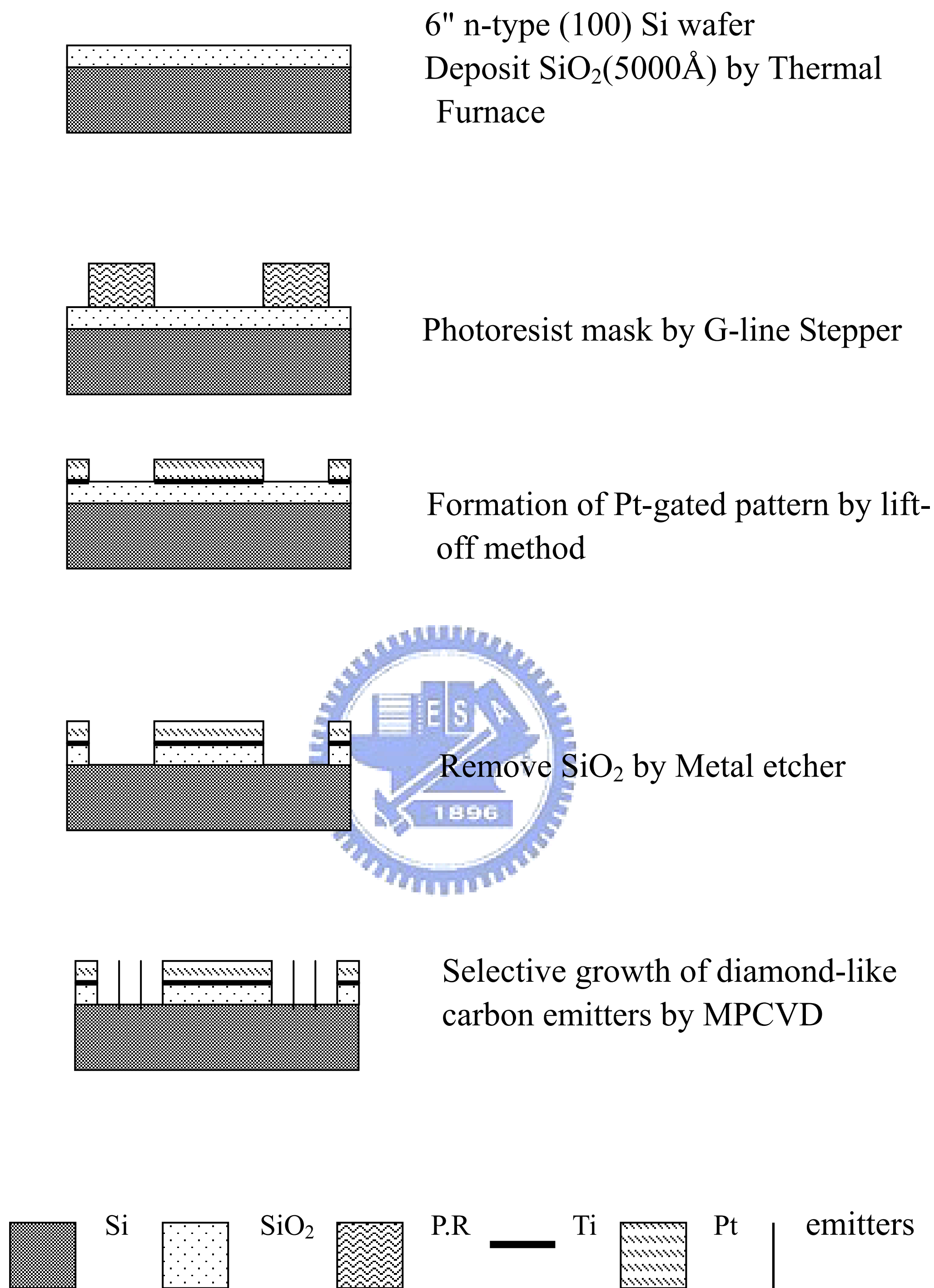

Fig. 5.1 Fabricated procedure of diamond-like carbon emitters on the FEAS with gated diode pattern.

technologies. Starting substrates were mirror-polish n-type, (100) oriented wafer with a resistivity of 4.5~5.5 Ω/cm. After fabricating the MIS diode, we put it in the bias assisted microwave plasma chemical vapor deposition (BAMPCVD) system to deposit diamond-like carbon emitters with various deposition parameters. Finally, several apparatuses analyzed the characterization of diamond-like carbon emitters.

5.2.1. Deposition of Silicon Oxide by Furnace and LPCVD System

The wafer was cleaned by RCA cleaning process to remove contamination on the silicon surface. After cleaning, SiO_2 layer of 500 nm thicknesses was deposited using a Furnace and LPCVD System (model ASM LB-45).

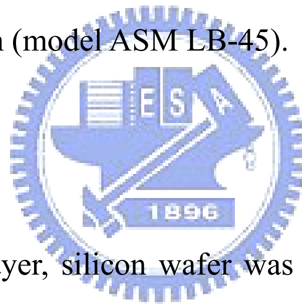

5.2.2. Lithography

After forming wet oxide layer, silicon wafer was covered with FH-6400 positive photoresist by using spin coater. A square of arrays of circle-shaped patterns was successfully fabricated after G-Line stepper (model ASM PAS 2500/10) exposing and developed (model Convac CPP-70) in the photoresist layer.

5. 2. 3. Deposition of Ti and Pt Films as Gated Layer using Dual E-Gun Evaporator

After forming photoresist patterns, adhesion between the Pt layer and SiO_2 layer was increased by sequentially depositing the Ti and Pt layers of 50 nm and 150 nm in thickness using Dual E-Gun Evaporator (model ULVAC EBX-10C, Japan). Table 5.1 summarizes those deposition conditions.

Materials	Ti(99%) and Pt(99.9%)
Layers of thickness	Ti (50 nm) and Pt (150 nm)
Before depositing pressure	1×10^{-6} Torr
Emission current	Ti(60 mA) ; Pt(150 mA)
Temperature	50 ~ 100℃
Deposition rate	0.1 ~ 0.2 nm/sec

Table 5.1 Conditions of deposited Ti and Pt layers.

5.2.4. Remove Photoresist by Lift-off Process

After the gated layers (Ti and Pt) formation, the photoresist was removed with an acetone solution in an ultrasonic agitator. The Pt-gated pattern with 4µm in diameter was formed by lift-off process. The distance between the 4µm-circle is 4µm, and the area with 50×50 circles is 0.396×0.396 mm^2. Figure 5.2 shows the SEM photograph of MIS diode structure of circle-patterns.

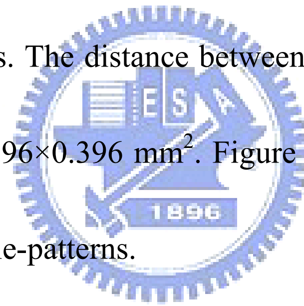

5.2.5. Removal of Silicon Oxide Layer by Metal Etcher System

Metal Etcher system (model ILD-4100 helicon wave etcher) was used to etch the SiO_2 layer with 500 nm depth after formation of a Pt-gated pattern by lift-off method. Finally, the FEA patterns were formed after these IC processes.

5.2.6. Diamond-like carbon emitters deposition condition

After fabricating the MIS diode, we put it in the bias assisted microwave plasma chemical vapor deposition (BAMPCVD) system to deposit diamond-like carbon emitters. The reactive gases used in deposition were the conventional mixtures of

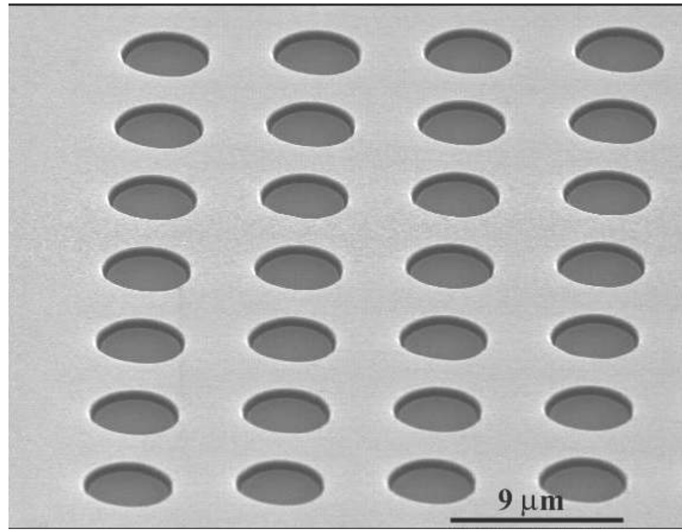

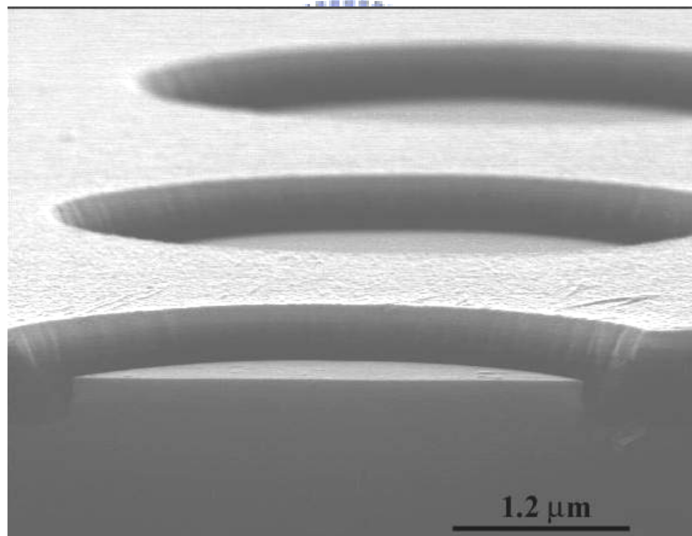

Fig. 5.2 SEM photographs of MIS diode structure with 50 x 50 circles.

CH_4-H_2 with trimethylphosphite $P(OCH_3)_3$ and trimethylborate $B(OCH_3)_3$ as the doping sources. All the experiments of the deposition used two-step depositions. The first step is employed as a nucleation process: the flow rates of CH_4/H_2 and deposition time remain constant at 10/200 sccm and 30 minutes, respectively. The second step is the growth process and the total deposition normally lasts for 60 minutes. While processing, the specimens were subjected to a negative bias voltage. Table 5.2 lists the experimental conditions. After processing, the product was to characterize the quality of the diamond material.

Table 5.2 Deposition conditions of undoped, boron and phosphours-doped DLC emitters, respectively.

Sample	First step flow rate CH_4/H_2+ doping source (sccm)	Second step flow rate CH_4/H_2+ doping source (sccm)
A (Undoped)	10/200	7.5/200
B (Undoped)	10/200	5/200
C (Undoped)	10/200	2/200
D (Phosphorus-doped)	10/200+2	2/200+2
E (Phosphorus-doped)	10/200+1	2/200+1
F (Phosphorus-doped)	10/200+0.5	2/200+0.5
G (Boron-doped)	10/200+2	2/200+2
H (Boron-doped)	10/200+1	2/200+1
I (Boron-doped)	10/200+0.5	2/200+0.5

First step deposition time = 30 min
Bias voltage = -130 V
MW power = 300 W
Doping source: $P(OCH_3)_3$ and $B(OCH_3)_3$

Second step deposition time = 30 min,
Total pressure = 2KPa
Substrate temp. (℃) = ~660

5.3. Results and Discussion

(I) SEM analysis

Figure 5.3 illustrates the undoped diamond-like carbon emitters grown under condition C. For the undoped emitters, the diamond nuclei are not observed when the negative bias voltage is below 80 V. Furthermore, the bias voltage of 90 V ~100V only grows tiny tips inside the hole. The higher bias voltage we apply, the more emitters we can obtain. This implies that the higher bias voltage enhances the growth of the emitters. Once we increase the bias voltage over 150 V, not only inside the hole but also on the Pt-gate was diamond. Indeed, the diamond may replace the Pt to form the diamond-gated field emissions arrays (FEAs). In the worst case scenario, this phenomenon will taint the I-V measurement because the field emission current maybe inexact because of the influence from both the diamond-like nano emitters and diamond-like-gated surface. Fig. 5.4 (a)~(c) show the undoped emitters grown under various methane concentration of the second step. As the concentration of methane increases, the amount of emitters increases. Under condition A, there are much diamond-like carbon nano particles embedded on the emitters. However, higher methane concentration also causes the Pt-gate to form some nano particles. This also influences the I-V measurement because of the previous reason. In this paper, the undoped optimize deposition condition is set as condition C. Undoped diamond emitters have several branches on their lateral or top directions. But from Figure 5.5

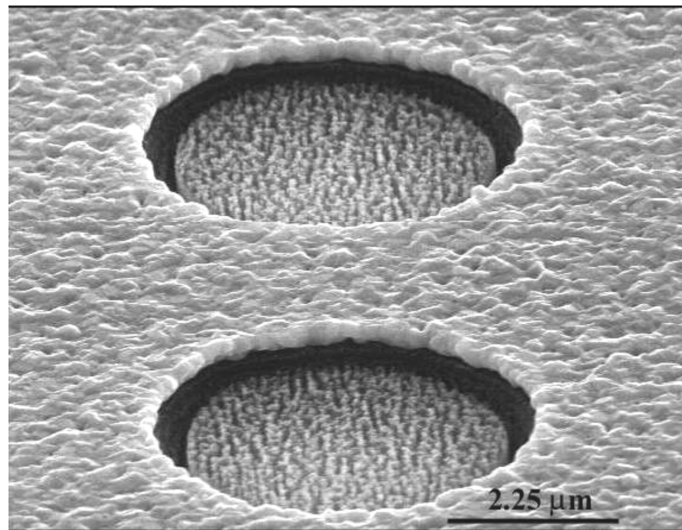

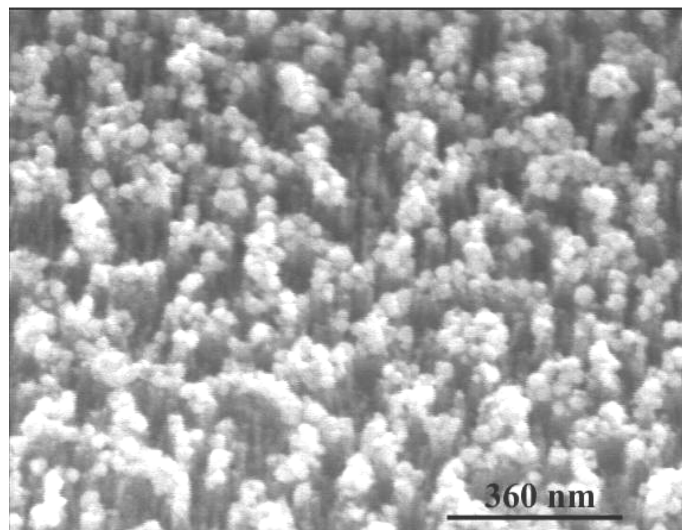

Fig. 5.3 SEM photographs of undoped diamond-like carbon emitters grown under condition C.

(a)

CH_4/H_2=10/200

CH_4/H_2=7.5/200

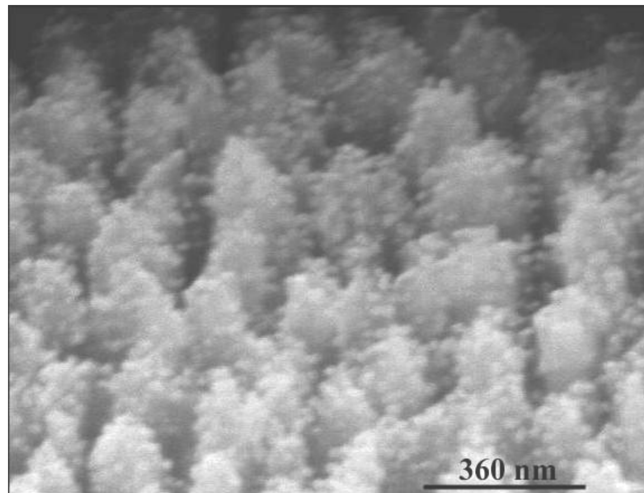

(b)

CH_4/H_2=10/200

CH_4/H_2=5/200

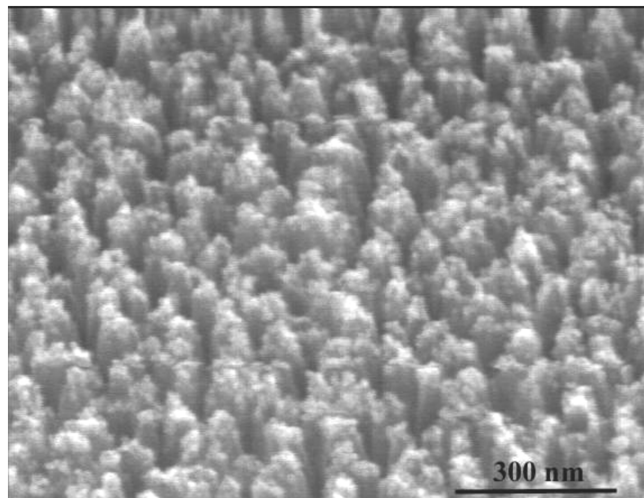

(c)

CH_4/H_2=10/200

CH_4/H_2=2/200

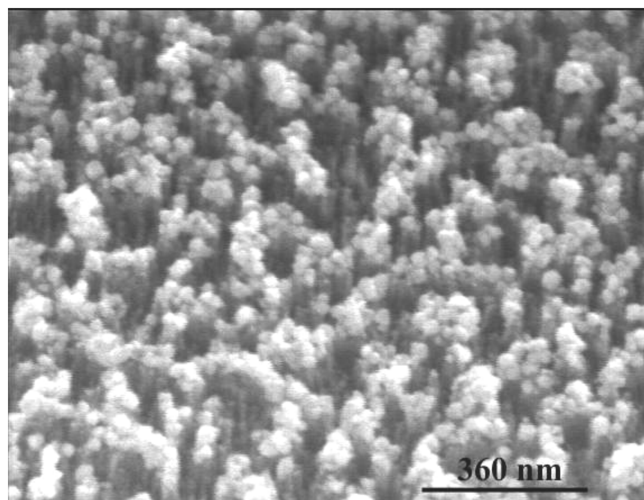

Fig. 5.4 SEM photographs of undoped diamond-like carbon emitters with various methane concentrations (a) sample A, (b) sample B and (c) sample C, respectively.

and Figure 5.6, the doping ones only have tiny tips around it. The most significant phenomenon is the quantity of diamond-like carbon emitters. Undoped diamond-like carbon emitters have higher growth rate than doping ones. The lower growth rate of the doped emitters could be explained by the following points. (I) $P(OCH_3)_3$ or $B(OCH_3)_3$ is a CH_3-rich compound that decomposes in plasma to produce an equal quantity of CH_3 radicals to balance the carbon source in the gas phase, thus the deposition rate will be reduced due to the increase of etching rate. (II) The lower growth rate of the doped samples is most likely due to the oxygen content contained in the $P(OCH_3)_3$ or $B(OCH_3)_3$. There were more oxygen atoms than phosphorus atoms in the doping source, which may be related to the etching of non-diamond carbon from the growing surface resulting in a lower growth rate. The same effects may also occur when adding O_2 to the CH_4-CO_2 gas mixture [7]. Additionally, many investigations have confirmed that phosphorus will lower the diamond growth rate in H_2-CH_4 mixtures [8].

(II) Raman Spectra

The microstructure and quality of the amorphous diamond-like carbon films were determined by Raman spectra. Raman measurements were performed at 514.5nm at $1cm^{-1}$ resolution, integration times were 1min at 30mW Ar ion laser power. Figure 5.7 gives the Raman spectrum of undoped diamond emitters. We can see there are

(a) $P(OCH_3)_3$ = 2 sccm

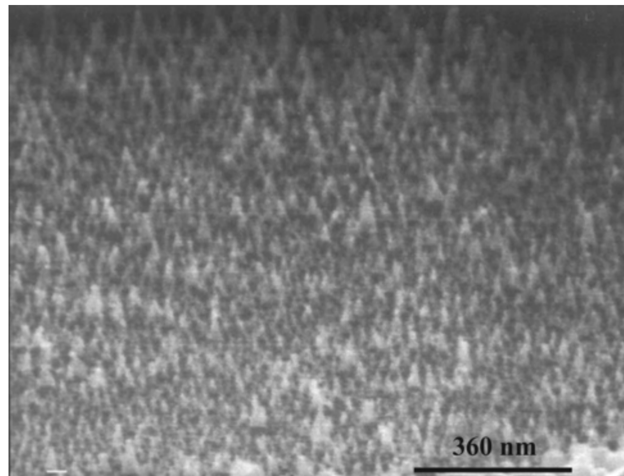

(b) $P(OCH_3)_3$ = 1 sccm

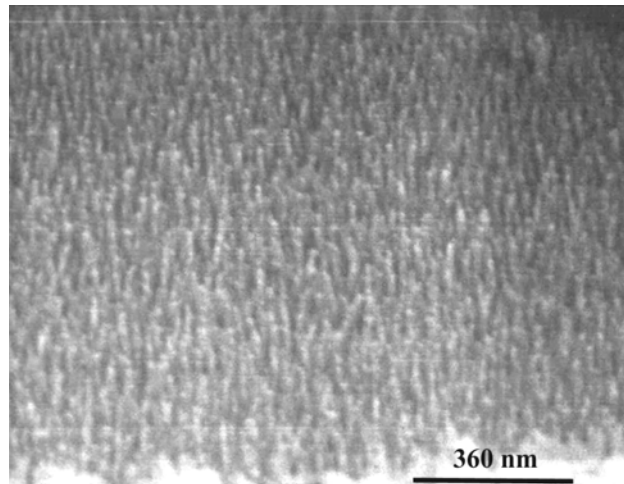

(c) $P(OCH_3)_3$ = 0.5 sccm

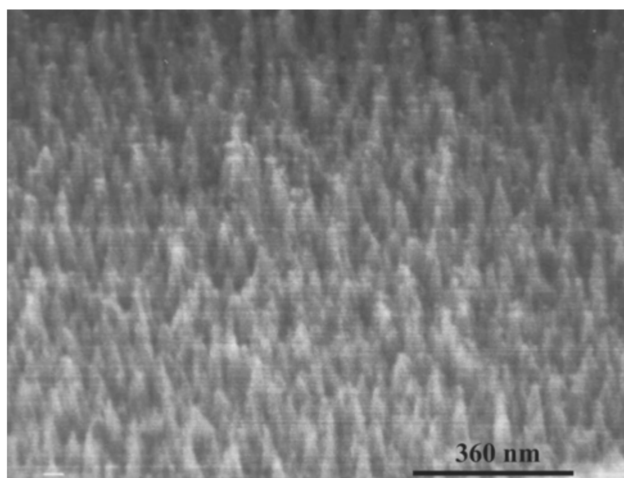

Fig. 5.5 The SEM photograph of phosphorus-doped diamond-like carbon emitters with various doping concentration (a) 2sccm, (b) 1sccm and (c) 0.5sccm, respectively.

(a) $B(OCH_3)_3$ = 2 sccm

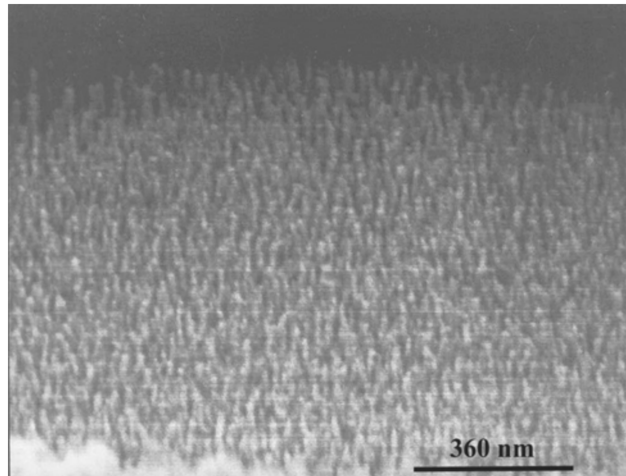

(b) $B(OCH_3)_3$ = 1 sccm

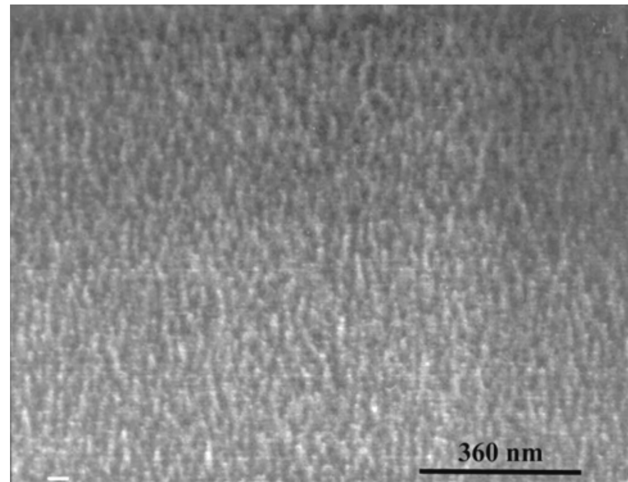

(c) $B(OCH_3)_3$ = 0.5 sccm

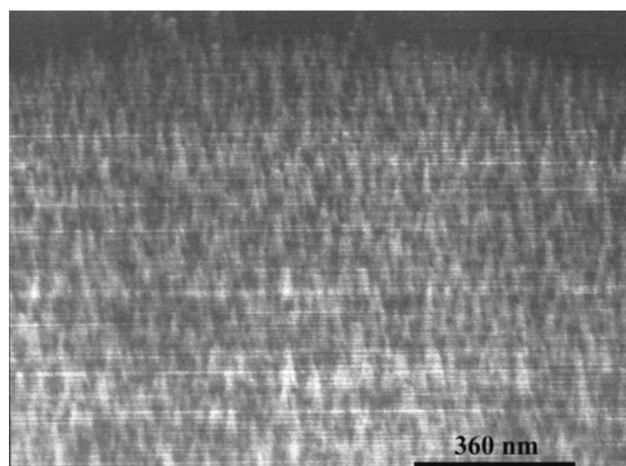

Fig. 5.6 The SEM photograph of boron-doped diamond-like carbon emitters with various doping concentration (a) 2sccm, (b) 1sccm and (c) 0.5sccm, respectively.

two obvious peaks located around 1350 cm^{-1} (D-band) and 1580 cm^{-1} (G-band). Normally a shark peak at 1332 cm^{-1} corresponding to the diamond zone center phonon line would be the principle Raman active feature in high quality crystalline CVD material. In this work, the spectral feature is diminished by stronger phonon bands attributable to diamond-like carbon (D-band) and crystalline graphite (G-band). This implies that the undoped emitters contain more graphitic material than diamond, and should strictly be classified as a diamond-like carbon (DLC) material. Figure 5.8 and 5.9 indicate that the graphitic content becomes even more dominant in the emitter material as the doping level of boron or phosphorus is increased. This observation is borne out by the fact that both doping gases are methyl-rich compounds. Thus, the etching rate declined while the quantity of amorphous carbon or graphite increased in the resultant films. A Raman shift occurs because of the internal stress in the diamond. This stress could be attributed to the following reasons: (I) the lattice mismatch between the diamond and phosphorus during growth; and (II) the thermal expansion coefficients of the diamond and substrate as well as the nanocrystalline nature of the diamond.

(III) Secondary ion mass spectrometry (SIMS)

Figures 5.10~5.11 show the depth profile of doped phosphorus and boron. The primary beam is O_2 with 8keV and 140nA. The rafter areas are 225 x 225 μm^2. Based

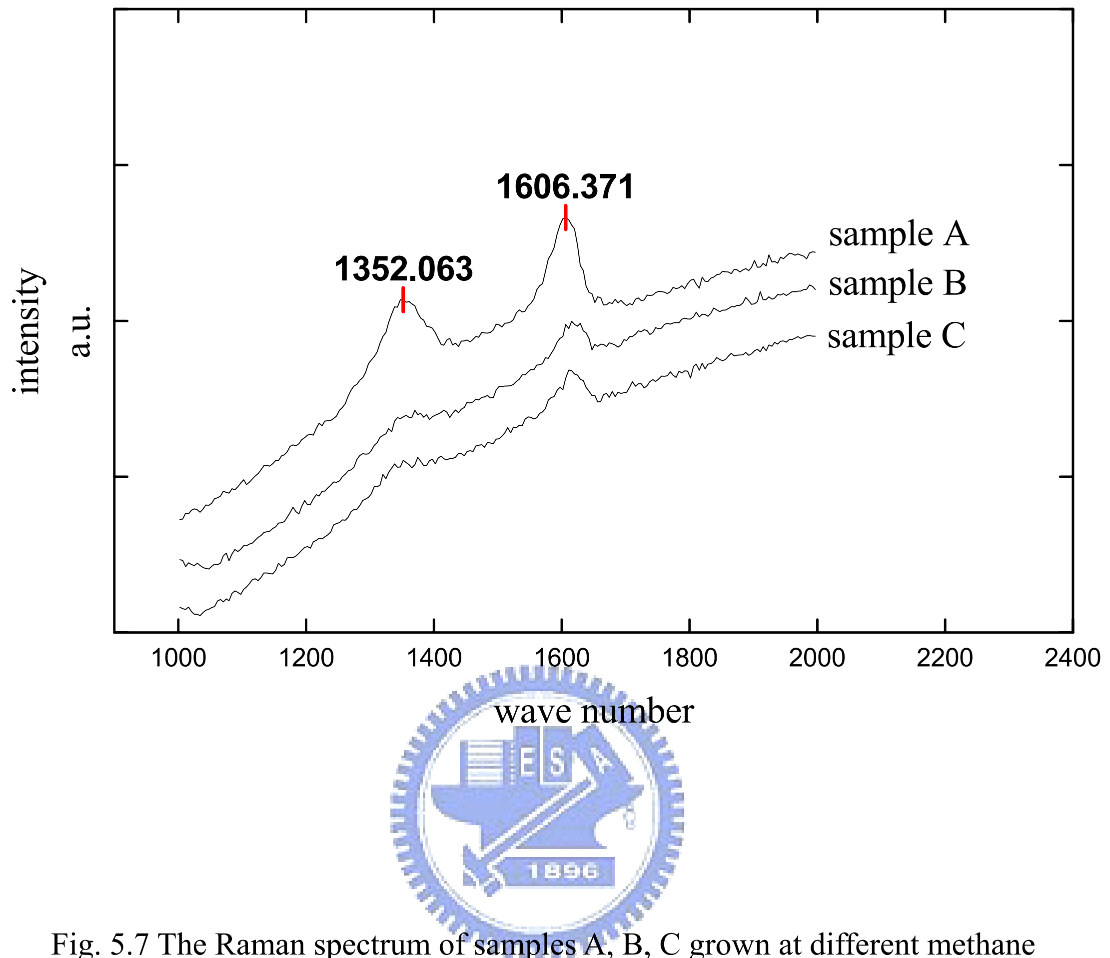

Fig. 5.7 The Raman spectrum of samples A, B, C grown at different methane concentration

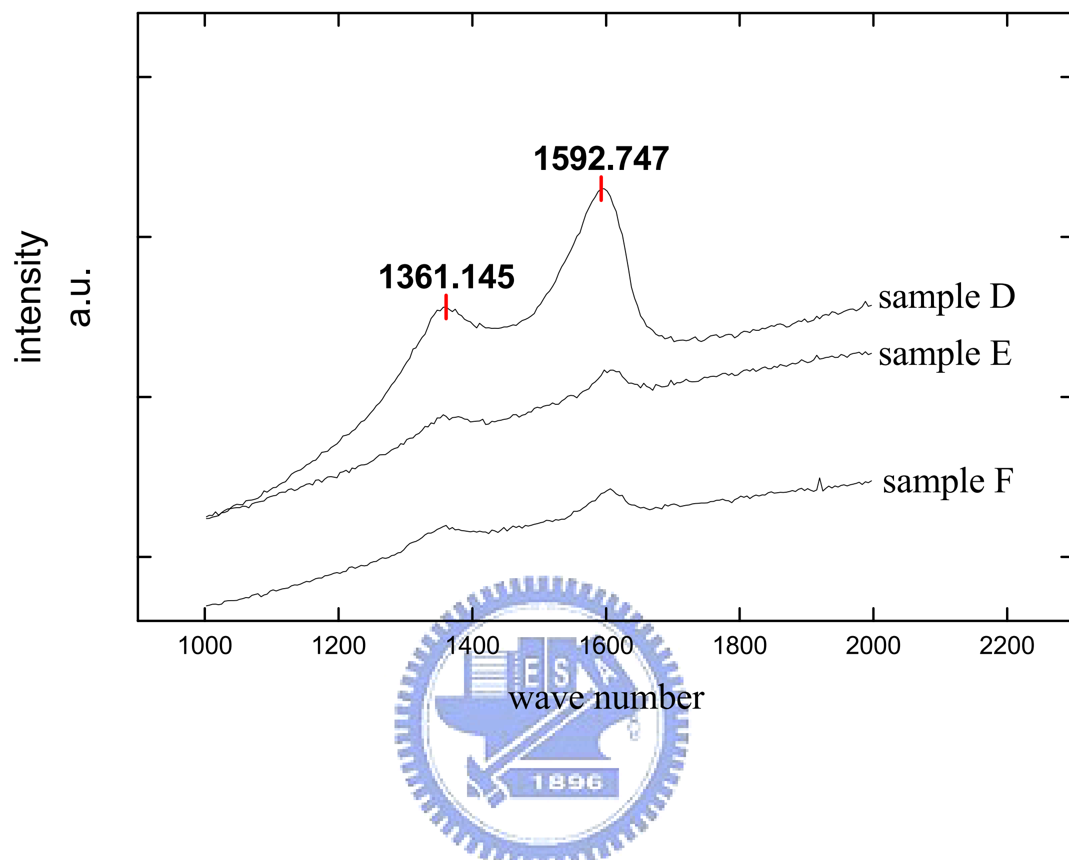

Fig. 5.8 The Raman spectrum of samples D, E, F grown at different phosphorus concentration

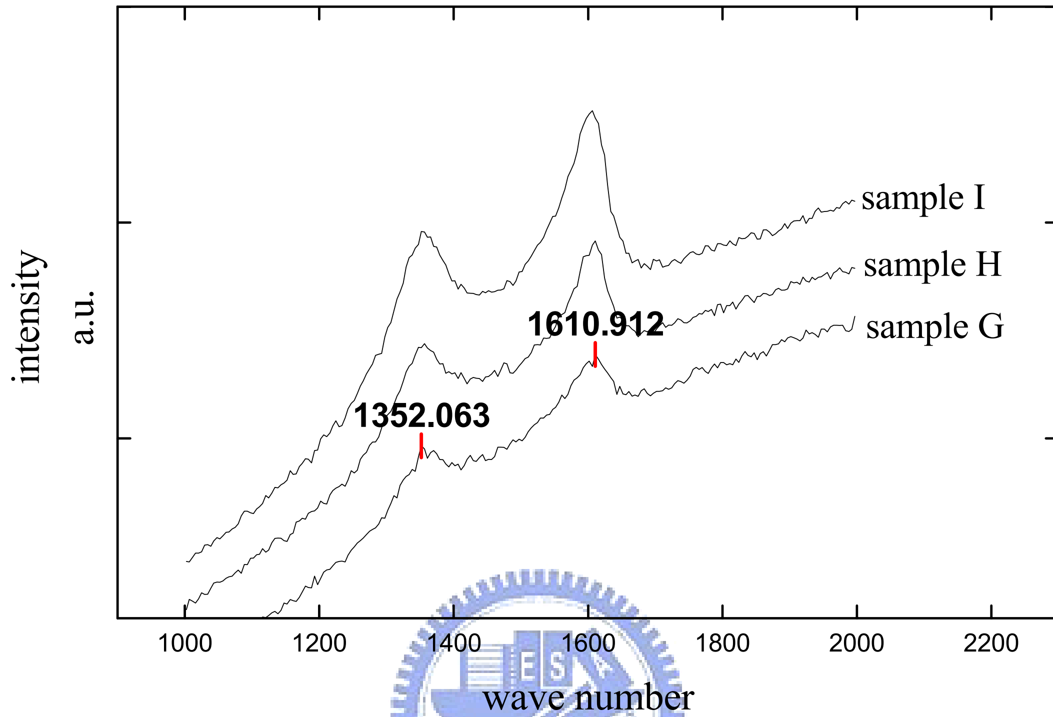

Fig. 5.9 The Raman spectrum of samples G, H, I grown at different boron concentration

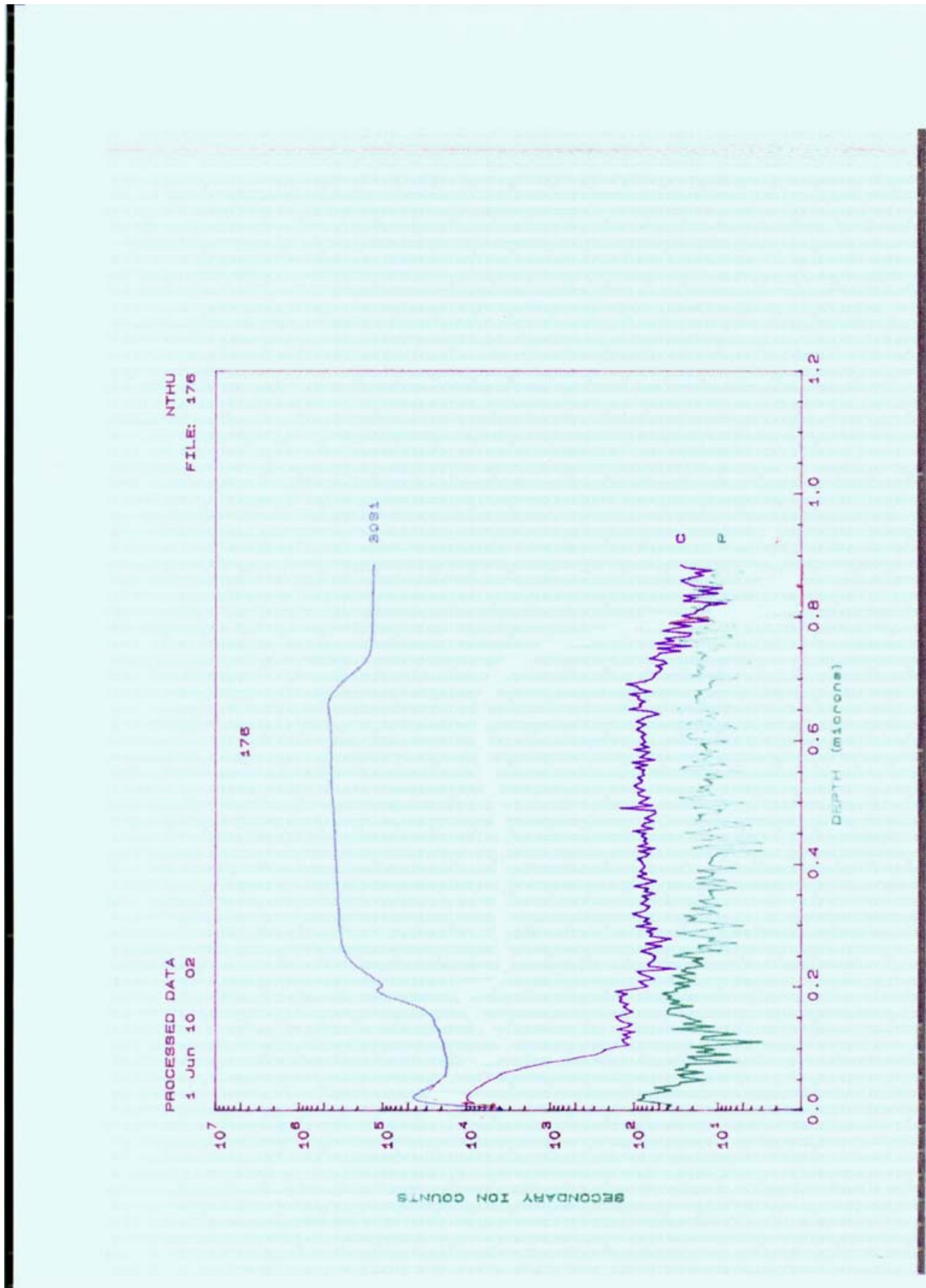

Figure 5.10 A SIMS depth profile of phosphorus (note: only qualitative analysis)

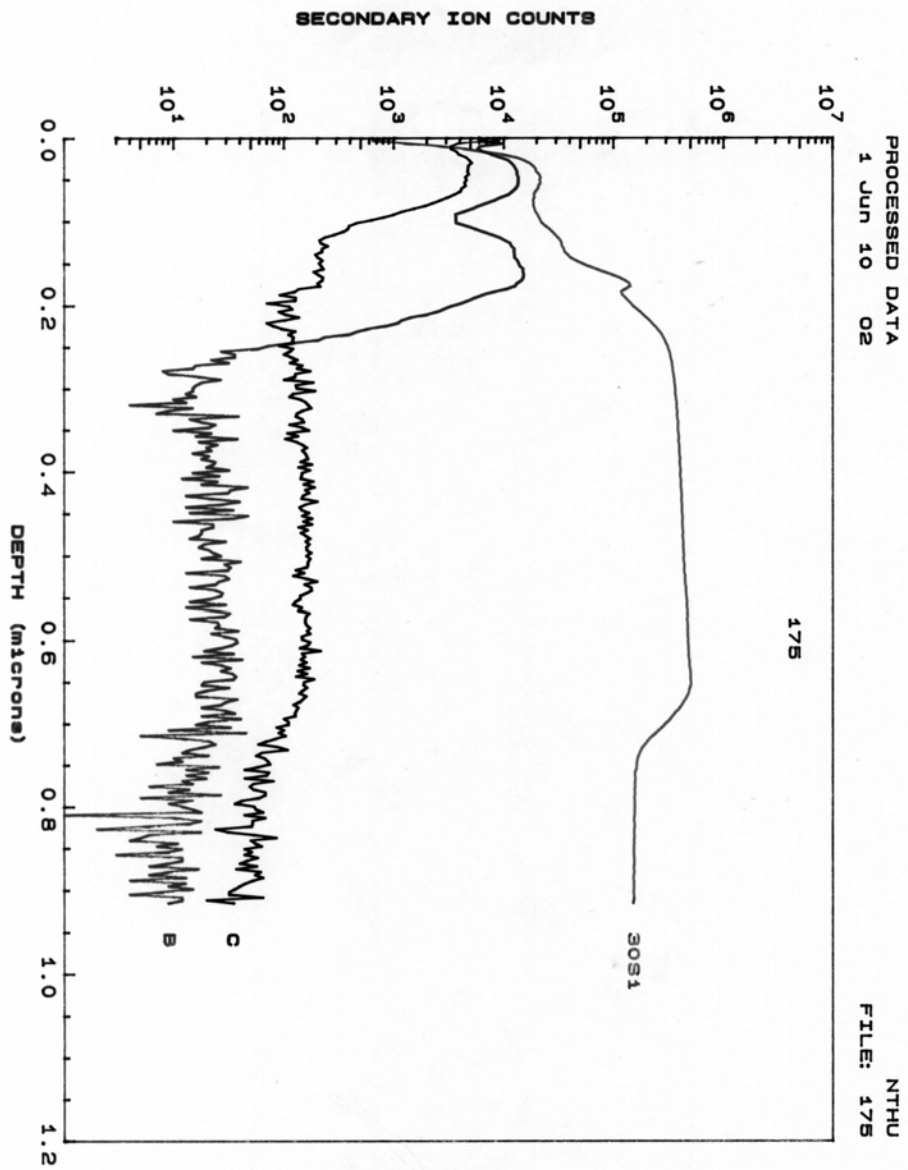

Figure 5.11 A SIMS depth profile of boron (note: only qualitative analysis)

on SIMS results, there are boron and phosphorus existing in the emitters clearly. It is worth noting that the SIMS detection is only qualitative analysis.

(IV) I-V measurement

Although diamond and diamond-like carbon (DLC) films have stable electron emissions at the low-field, the nature of electron emission from these materials remains unclear [9]. We are currently employing different approaches to explain the ultra-low emission fields. Many factors affect the field emission characterization of diamond including impurity, and defect levels [10] in the diamond band gap; hot electron transport in interfaced structures [11]; grain boundary effects [12]; and geometric field enhancement (β) by morphology protrusions or narrow conductive grain boundaries between insulating grains. In this paper, there are significant differences between phosphorus and boron doping. Figure 5.12 shows the field emission current density (J_e) of undoped; boron-doped and phosphorus-doped diamond-like emitters with 0.013; 0.24 and 1.03 A/cm^2. The currents of boron-doped and phosphorus-doped emitters are twenty and eighty times larger than the undoped one. The electron emitting properties were further evaluated by the Fowler-Nordheim plot shown as an insert to figure 5.12.

The experimental results confirm that phosphorus-doped emitters have a better field emission property than boron-doped for the following reasons. Doping with

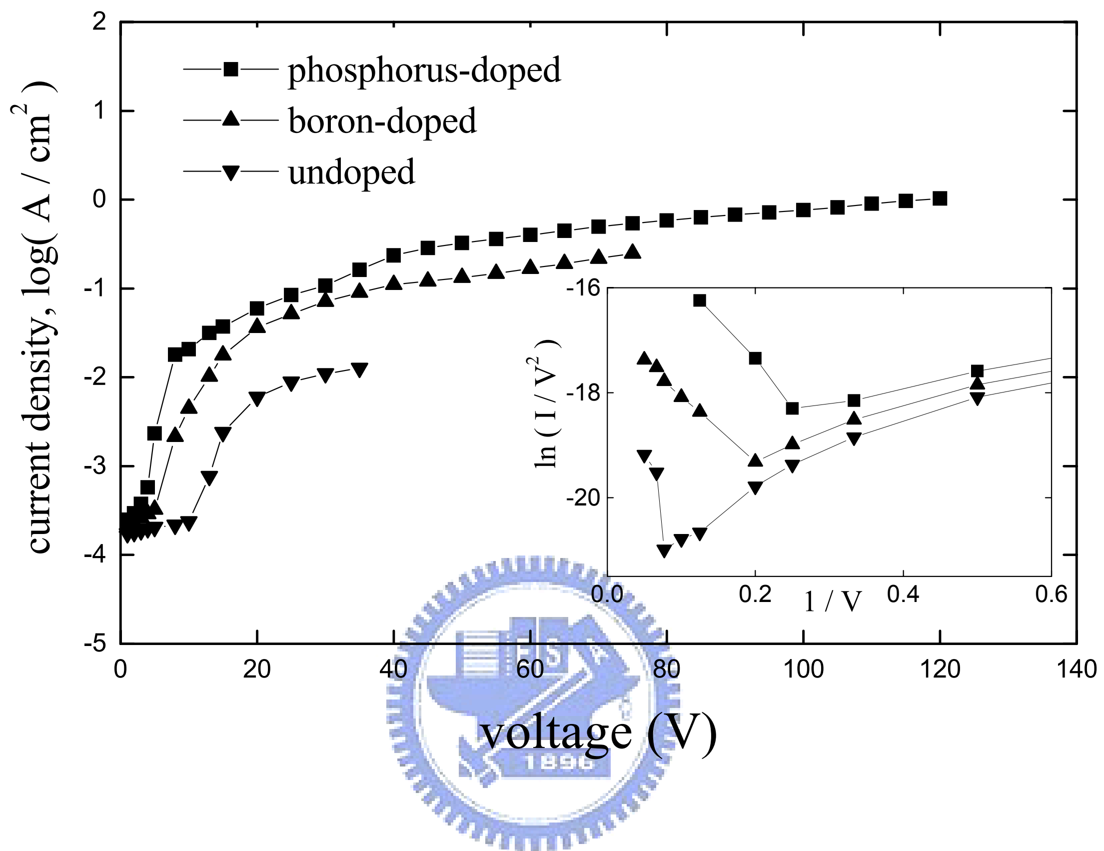

Fig. 5.12 The J_e-V curve of undoped; phosphorus-doped and boron-doped diamond emitters and an insert of Fowler-Nordheim plot.

phosphorus has substantially more influence on conductivity than doping with boron. The other is due to the morphology of the emitters' structure. Phosphorus also provides its conduction electrons with more opportunity to be extracted because ionized donors form a space charge layer [13]. Solid-state physics indicates that doping boron or phosphorus will instigate an energy band modification in the material by generating a donor or acceptor level that provides more electrons or holes for the material. These increase the total conductivity and net flux of carriers.

The field emission property of diamond can be enhanced by increasing the sp^2 content because of the following reasons:

(I) The defect-induced band created by the sp^2 content.

The defect-induced energy band created by the sp^2 content is responsible for the field emission enhancement. A defect-induced energy band can be induced throughout the diamond energy gap in response to the presence of a wild variety of structural defects created as a consequence of the sp^2 particles. The formation of these defect bands raises the Fermi level toward the conduction band, and thus reduces the work function for enhancing field emission.

(II) The field enhancement factor is increased by the sp^2-diamond-sp^2 microstructures.

Conducting sp^2 particles in isolated diamond form cascaded sp^2- diamond-sp^2 (MIM) microstructures which could enhance the field enhancement factor. The field

enhancement factor ß is affected by the following geometrical parameters of the device structure: the gate opening diameter, tip radius, emitter high and tip position with respect to the center of the gate thickness and the emitter morphology. Adding phosphorus or boron changes their structures and also affects the field enhancement factor ß.

There is a saturated current at Vgc=40V; 77V and 120V in non-doped, B-doped, and P-doped diamond emitter arrays. This saturation can be accounted for in two ways: the tip effect of the diode structure. The far distance between Pt-gated and the diamond–tip depends on the size of the diamond tip and the aperture depth. Thereby, part of the field emission current that flows into the Pt-gated and the anode current is reduced. The other reason is the dielectric layer (SiO_2) in the developed pattern may be broken which will create a leakage current when high voltage is applied.

5.4. Conclusion

In this paper, we synthesized phosphorus-doped and boron-doped emitters by using trimethylphosphite $P(OCH_3)_3$ and trimethylborate $B(OCH_3)_3$ as doping sources. Undoped emitters have higher growth rate than doping ones. The lower growth rate of the doped emitters could be explained by the following points. (I) $P(OCH_3)_3$ or $B(OCH_3)_3$ is a CH_3-rich compound that decomposes in plasma to produce an equal quantity of CH_3 radicals to balance the carbon source in the gas phase, thus the

deposition rate will be reduced due to the increase of etching rate. (II) The lower growth rate of the doped samples is most likely due to the oxygen content contained in the $P(OCH_3)_3$ or $B(OCH_3)_3$. Doping both phosphorus and boron can enhance electric properties by reducing the turn-on voltage and can increase the emission current density. The emission current densities of boron-doped and phosphorus-doped emitters are about twenty and eighty times larger than the undoped.

5.5 Reference

1. M.W. Geis, N. N. Efremow, J. D. Woodhouse, M.D. McAleese, M. Marchywka, D. G. Socker , and J.F. Hochedez , IEEE Electron Device Lett 12,456 (1991)

2. C. Wang, A. Garcia, D. C. Ingram, M. Lake, M. E. Kordesch, Electronics Lett. 27,1459 (1991)

3. N.S. Xu, Y. Tzeng, and R. V. Latham, J Phys. D26, 1776 (1993)

4. K.Okano, K. Hoshina, M. Iida, S. Koizumi, and T. Inuzuka, Appl.Phys Lett.64, 2742 (1994)

5. H. K. Schmidt, M. H. Clark. I. Yee, and N. Kumar, Abstract for the SID Manuf. Conference, 1994.p.21.

6. C.F. Chen, H.C. Wang and H.C. Hsieh, Jpn. J.Appl.Phys.Vol.39, 1880-1884 (2000).

7. C. F. Chen, T. M. Hang and S. H. Cheng, J Appl. Phys, 74 4483 (1993)

8. S. N. Schauer, J. R. Flemish, and R. Wittstruck Appl. Phys. Lett. 64 (9)1094 (1994)

9. J.Ristein, Diamond Relat. Mater. 9,1129, (2000).

10. W. Zhu, G. P. Kochanski, Mat. Res. Soc. Proc., Vol. 416, 443 (1996).

11. N. M.Miskovsky, P. H. Cutler, Z-H. Huang, P. D'Ambrosio, P. Lerner, Mat. Res. Soc. Symp. Proc., Vol. 416, 437, (1996).

12. A. V. Karabutov, V. D. Frolov, S. M. Pimenov, V. I. Konov, Diamond Relat. Mater. 8, 763, (1999).

13. K. Kuriyama; C.Kimura, S. Koizumi, M.Kamo and T. Sugino. J. Vac.Technol. B 17 (2) 723 (1999)